ISSN 1063-7842, Technical Physics, 2015, Vol. 60, No. 4, pp. 575–582. © Pleiades Publishing, Ltd., 2015.
Original Russian Text © V.O. Gladyshev, D.I. Portnov, 2015, published in Zhurnal Tekhnicheskoi Fiziki, 2015, Vol. 85, No. 4, pp. 97–104.

OPTICS

# Evolution of the Polarization of the He–Ne-Laser Radiation in a Rotating Insulator

**V. O. Gladyshev* and D. I. Portnov**

*Bauman State Technical University, Vtoraya Baumanskaya ul. 5, Moscow, 105005 Russia*
**e-mail: vgladyshev@mail.ru*

Received June 5, 2014

**Abstract**—The propagation of the polarized coherent radiation of a He–Ne laser in a rotating insulator is experimentally studied. The reversible transient process of the rotation of the polarization plane and variations in the degree of ellipticity, depolarization, and deflection of the laser beam with a relaxation time of $\tau = 10^2$–$10^3$ s are observed at an insulator rotation frequency of $f = 2$–$250$ Hz.

**DOI:** 10.1134/S106378421504012X

## INTRODUCTION

The propagation of a linearly polarized plane monochromatic electromagnetic wave through a rotating isotropic insulator with refractive index $n$ is accompanied by the rotation of the polarization plane. The polarization rotation angle must be proportional to the time of the wave passage through the medium $t = nl/c$ and the Fresnel drag coefficient $\alpha = 1 - 1/n^2$.

This effect can be used for the study of the rotational motion of medium that transmits radiation. In addition, the analysis of the propagation of the electromagnetic radiation in a rotating insulator will make it possible to solve the problem of lasing in media with relatively low thermal conductivities. From the practical point of view, a variation in the polarization state in an optically transparent disk allows the control of laser radiation. Such a technology can be used to control the coherent radiation of any laser, since optically transparent media are available for different (from UV to far-IR) spectral ranges.

The rotation of the polarization plane of a monochromatic electromagnetic wave that is incident along the normal on a rotating homogeneous isotropic insulator has been predicted in [1]. The rotation of optical medium must lead to the polarization rotation of the radiation having passed through the rotating disk or cylinder by the angle that linearly depends on rotation frequency $f$ and optical path in the medium $L = nl$. In the experimental measurement of this effect in [2], the laser radiation was incident almost along the normal on the plane surface of a cylindrical rod with a length of 100 mm and a diameter of 20 mm. Such an effect has not been studied at different angles of incidence.

The calculations yield relatively small angles of polarization rotation of coherent radiation (several microradians), which accounts for the complexity of the experimental study and limitations on the practical applications of this classical electrodynamic effect of moving media. The analysis is performed under the assumption that the optically transparent cylinder is homogeneous and isotropic in the course of rotation. Such an assumption is valid with a certain accuracy, since the rotation-induced anisotropy of optical properties can be observed at relatively high rotation rates.

The resulting stresses lead to the birefringence and variations in the polarization state. We may assume that the polarization rotation of an electromagnetic wave is proportional to the square of the angular velocity of the insulator. However, the experiments of [3] yield a nonlinear dependence of the rotation angle of polarization plane on the rotation frequency of insulator. In this work, we study time- and frequency-dependences of the polarization rotation angle, ellipticity, degree of polarization, and angular characteristics of radiation propagating through a rotating insulator that exhibits isotropy and optical transparency at rest.

## EXPERIMENTAL SETUP

In the experiments, the radiation of the LGN 302 laser passes through a rotating optical disk (OD) that is made of the TF3 glass with a refractive index of $n = 1.71233$ at a laser wavelength of $\lambda = 0.63$ μm (Fig. 1).

The radiation is incident on the plane surface of the disk at an angle of incidence of $\vartheta = 60°$. The OD diameter is $2R_0 = 62$ mm (Fig. 1), and the thickness is $d = 10$ mm. Reflecting metal coatings with radius $R_1$ on the plane OD surfaces provide an increase in the optical path. The number of rereflections at the plane mirrors deposited on the OD surfaces is $N = 6$ (for simplicity, Fig. 1 shows only four reflections). The total optical path of the beam that propagates from point $A$ to point $B$ at $N = 6$ is $L = (N + 1)nl = 139$ mm. It is seen that the OD represents a plane-parallel plate in the transmission configuration.

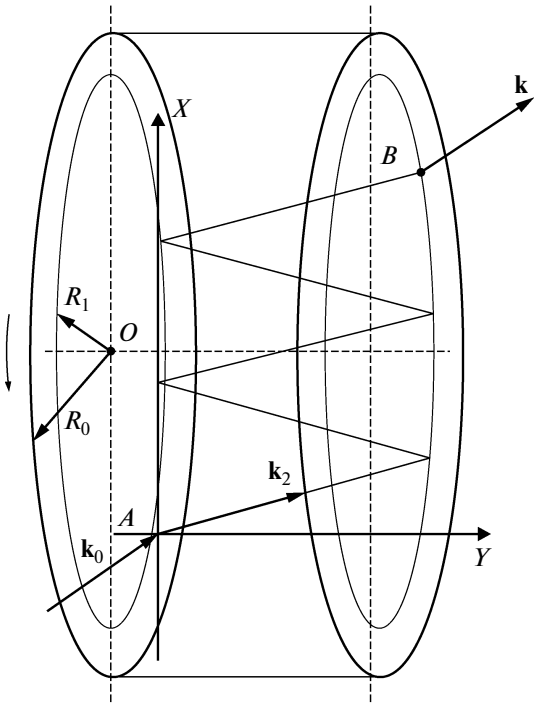


**Fig. 1.** The optical scheme of the disk under study. The beam is refracted at point *A*, reflected from the mirrors with radius $R_1$ on the plane OD surfaces, and leaves the disk at point *B*. Wave vector **k** of the transmitted electromagnetic wave is collinear to wave vector $\mathbf{k}_0$ of the incident wave.

Figure 1 shows the top view. The horizontal plane in which the beams are rereflected at plane mirrors on the disk is located at a distance of 20.5 mm above the rotation axis. The geometrical optical path corresponds to the maximum beam dragging (i.e., the angle of incidence and the path length are such that the maximum Fizeau effect and deviations from the Snell law are reached). The problems of the optimal propagation of the beams in OD that provides the maximum effect of the optics of moving media on the propagation of the coherent electromagnetic radiation in the rotating OD have been studied in [4].

Figure 2 presents the experimental scheme. We use laser *L* (LGN 302 laser) that generates radiation with a power of 0.7 mW in each of two linearly polarized orthogonal components. Polarizer *P*1 makes it possible to choose the horizontal or vertical linearly polarized component with the single-frequency regime in each polarization. Laser wavelengths in vacuum $\lambda_1 = 0.6329910$ μm and $\lambda_2 = 0.6329918$ μm correspond to the high- and low-frequency components, respectively. The radiation passes through optical system *OS*1 that contains a pinhole and is divided by beamsplitter *BS* into two beams that propagate in the ring scheme along opposite directions. The beams reflected from mirrors *M*1 and *M*2 pass through optical disk *OD* and beamsplitter *BS*. The beams that leave the ring scheme pass through polarizer *P*2 and optical system *OS*2

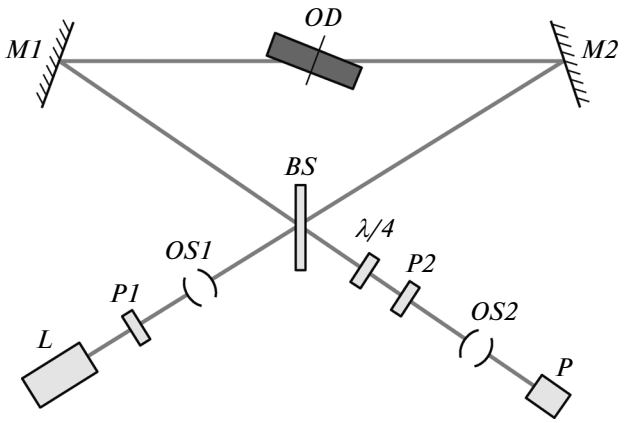


**Fig. 2.** Optical scheme of the setup. The beams propagate through optical disk *OD* in opposite directions. Polarizer *P*2 is used to determine the polarization rotation angles. The λ/4 retardation plate makes it possible to determine the ellipticity of the radiation having passed through the *OD*.

(negative lens) and arrive at photodetector *PD*. The λ/4 retardation plate is placed in front of polarizer *P*2 and used to determine the ellipticity of the radiation having passed through *OD*.

The polarization of the laser radiation having passed through *OD* is independently determined using the Glan–Taylor prism and a film polarizer. The OD is rotated by a three-phase induction motor that is controlled by the Delta Electronics VFD-EL digital frequency converter. The output radiation is detected using a fast photodiode with a bandpass preamplifier. The signal of the photodetector is processed using a 14-bit ADC.

The ring optical scheme with the rotating optically transparent disk is used to study the optical effects in moving media. Such an experimental configuration makes it possible to study both the polarization characteristics of the radiation having passed through the rotating insulator and the Fizeau effect the measurements of which employ the interference signal.

The effects of longitudinal and transverse dragging of a plane monochromatic electromagnetic wave in a moving insulator have been studied in earlier experiments with a disk interferometer with allowance for violations of the Snell law at the tangential discontinuity of the velocity [4]. The tangential discontinuity of the velocity emerges at the interface of the optically transparent medium (disk or cylinder) that rotates around the symmetry axis. The above experimental scheme makes it possible to separately study the amplitude and phase characteristics of the two beams having passed through the disk in opposite directions. In this work, we study the polarization of the laser radiation and demonstrate the similarity of the characteristics depending on the rotation frequency for a single laser beam having passed through the rotating disk and the interference of two beams having passed

through the disk in opposite directions. The effect of polarization on the interference signal is needed for the analysis of the Fizeau effect and the remaining effects of optics of moving media.

## DEPENDENCE OF THE SIGNAL AMPLITUDE ON THE OD ROTATION FREQUENCY

In the experiments, we measure the amplitudes of the PD signals and rotation angle of polarization plane $\Delta\varphi(f_i)$ at different rotation frequencies $f_i$ of the OD. First, we choose the polarization of the incident beam using polarizer $P1$. In the steady-state regime of the laser, we determine the polarization of radiation having passed through the OD at rest and fix the rotation angle of polarizer $P2$ that provides the minimum output signal. In this case, the PD signal is no greater than the noise level at any angular position of the OD. This result is possible if the OD does not have internal stresses, which may lead to depolarization of radiation. Thus, the radiation having passed through the OD at rest is linearly polarized and the signal related to the OD rotation is absent. Then, we measure the first value of the signal amplitude at different rotation frequencies $f_i$ at this position of the second polarizer.

The OD reaches the predetermined rotation frequency with a delay of 60 s relative to the moment at which the gyromotor is switched on. When the rotation is started, the polarization is rotated and we obtain the PD signal that corresponds to the radiation having passed through polarizer $P2$. In the experiments, we measure the amplitude at the maximum of the time signal. The signal is recorded at a sampling rate of 100 kHz that is sufficient for the detailed observation and control of the shape of the time signal. Note that the rotation- induced signal may depend on the stresses in the disk material but this problem needs to be further investigated.

To determine rotation angle $\Delta\varphi_i$ of the polarization plane for rotating OD, we rotate polarizer $P2$ to minimize the transmitted intensity. In this case, the radiation is not linearly polarized. Then, we compare the measured pairs of signal amplitudes corresponding to the initial position of the polarizer and the polarizer rotation to the minimum signal. The measurements are performed in the frequency interval $f = 100$–220 Hz with a step of 10 Hz.

Figure 3 shows the measured amplitudes of the PD signals for the initial vertical polarization of the laser radiation. The polarizer rotation leads to a decrease in the signal from 50 to 25 mV at a rotation frequency of $f = 220$ Hz.

The OD reaches the predetermined rotation frequency with a delay of 75 s, so that the time interval between the measurements at different frequencies is 100 s. Thus, the experimental results can not be used to characterize the transient processes of variations in the polarization state at fixed frequency $f_i$, since the characteristic times of such processes are significantly longer.

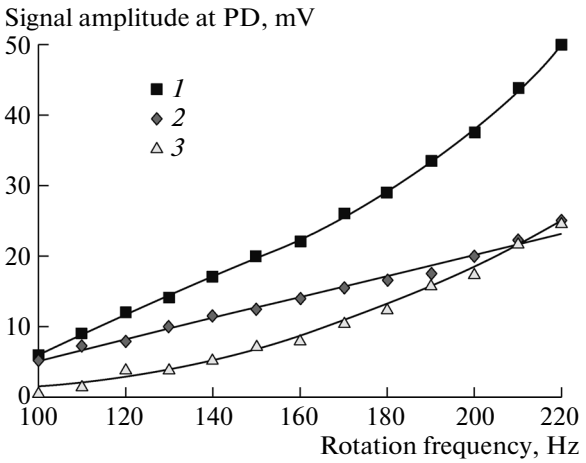


**Fig. 3.** Plots of the PD signal amplitude vs. OD rotation frequency for the spectral component of the vertical polarization for (*1*) the initial position of the polarizer and (*2*) the polarizer position that corresponds to the minimum signal and (*3*) the difference of the two curves.

The results show that an increase in the OD rotation frequency leads to an increase in the amplitude of the PD signal. The data also show that rotation of the second polarizer does not allow a decrease in the signal to the noise level upon the steady-state rotation of the OD. The experimental results indicate the presence of rotation-induced birefringence in the OD, so that the initially linearly polarized radiation is transformed into the elliptically polarized radiation. This assumption is proven by measurements that are performed in accordance with the GOST R50006-92 standard in the presence and absence of the $\lambda/4$ retardation plate (the plate is placed in front of polarizer $P2$).

Figure 4 shows the calculated ellipticity angles $\varepsilon$ that are obtained using the experimental data and the smoothed curve $\varepsilon(f)$.

The ellipticity is measured as the ratio of minor axis $b$ of the polarization ellipse to major axis $a$:

$$e = \frac{b}{a} = \sqrt{\frac{I_{\min}}{I_{\max}}} = \sqrt{\frac{1-p}{1+p}}.$$

Here, $p$ is the degree of polarization and $I_{\max}$ and $I_{\min}$ are the minimum and maximum intensities, respectively, that are measured at different angular positions of the polarizer.

At a time delay of 15–30 min relative to the beginning of the rotation, the measurements in the absence of the $\lambda/4$ plate yield ellipticities $e = 0.25$, 0.36, 0.23, and 0.15 for frequencies $f = 5$, 30, 80, and 200 Hz, respectively. The corresponding ellipticity angles are $\varepsilon = \tan^{-1}e = 14.3°$, 19.9°, 12.7°, and 8.4°. In the presence of the $\lambda/4$ retardation plate, the ratio of the semiaxes can be decreased. For example, the ellipticity decreases to $e = 0.2$ ($\varepsilon = 11.3°$) for the initially hori-

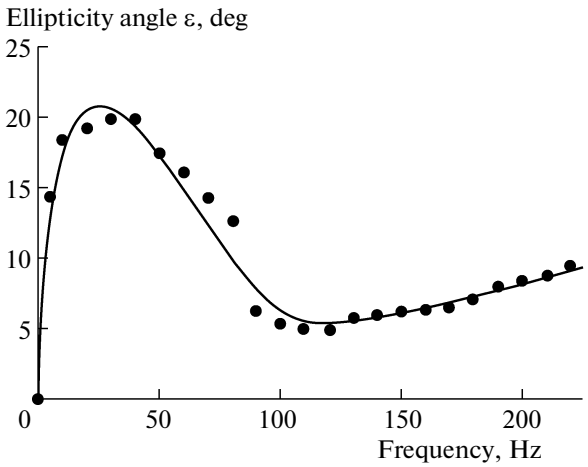


**Fig. 4.** Plots of ellipticity angle ε vs. rotation frequency *f*. The curve contains a nonlinear fragment in the frequency interval 0–100 Hz.

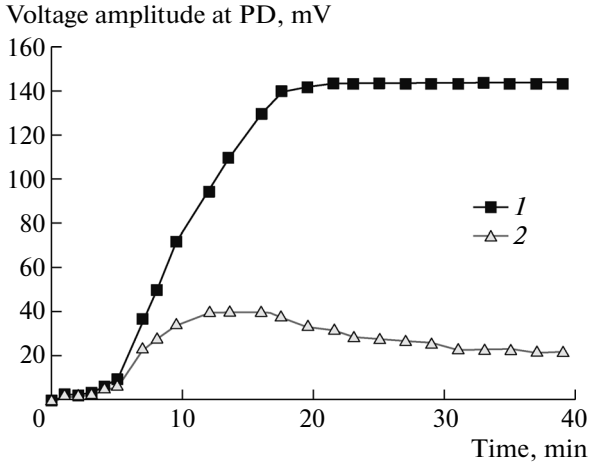


**Fig. 5.** Plots of the maximum PD voltage amplitude vs. time at a rotation frequency of 50 Hz for the horizontal spectral component: (*1*) signal amplitude for the initial position of the polarizer and (*2*) signal amplitude after the polarization rotation to the signal minimum.

zontal linear polarization and an OD rotation frequency of $f = 30$ Hz. The nonzero ellipticity indicates that the birefringence in the rotating disk is supplemented with the depolarization. The degree of polarization is estimated to be $p = 0.9$ at a frequency of $f = 30$ Hz. For the OD at rest, the ellipticity is $e = 0$ and the degree of polarization is $p = 1$. Curve *2* in Fig. 3 is close to a straight line, so that a combination of ellipticity and depolarization linearly depends on the angular velocity. Multiple measurements at different days yield a relatively high reproducibility of the dependence of the PD-signal amplitude on rotation frequency *f*.

## EVOLUTION OF THE POLARIZATION OF RADIATION HAVING PASSED THROUGH THE ROTATING INSULATOR

The preliminary experimental results show a slow drift of the rotation angle of the polarization plane in time at a rate that depends on disk rotation frequency *f*.

Such an effect was studied at frequencies of up to 250 Hz. In the experiments, the time dependence of the polarization rotation was separately measured for two beams for vertical and horizontal spectral components of the laser.

Prior to the measurements, one beam is tuned in such a way that the maximum signal intensity (bright part of the spot) is delivered to the PD aperture. Then, the polarizer is rotated to minimize the transmitted signal. Such a position of the polarizer is used as the initial position.

For the steady-state rotation of the disk, we start from the measurement of the signal amplitude at the maximum of the time dependence of the PD voltage at the initial position of polarizer *P*2. In such measurements, we provide the maximum intensity on the PD aperture. Then, the signal amplitude is measured after the rotation of the polarizer by the angle that is determined by the polarization rotation of the beams (the polarizer is rotated to minimize the signal). Then, the prism is rotated to the initial position and the measurements are repeated with a time interval of 5 min.

Figure 5 shows the experimental results for a frequency of $f = 50$ Hz. The curve of the maximum PD voltage amplitude versus time exhibits saturation (curve *1*). With a delay of 20 min relative to the beginning of the measurements, the signal amplitude at the maximum of the time response appears to be greater than 140 mV and, then, remains almost unchanged.

Curve *2* shows the dependence of the PD voltage amplitude for the polarizer that is rotated to the signal minimum. Note the nonmonotonic character of the dependence.

Curve *1* characterizes the simultaneous effect of the polarization rotation and variation in the degree of ellipticity and depolarization. Curve *2* characterizes the time dependence of ellipticity and depolarization. Curve *2* shows that a variation in the degree of ellipticity with time exhibits an extremum at a time of about 13 min after the beginning of the measurements for the given rotation frequency. Such nonmonotonic behavior is observed only at the frequencies $f \le 60$ Hz. At the frequencies $f > 60$ Hz, the exponential growth of the PD voltage is observed [3].

We also measured the polarization rotation angle over an interval of 140 min. The experiments show that at the frequency $f = 50$ Hz angle $\Delta\varphi$ reaches the saturation level at a time of 20 min and, then, remains unchanged.

Figure 6 presents the time dependence of rotation angle $\Delta\varphi$ of polarization plane at a rotation rate of $f = 80$ Hz. It is seen that polarization rotation angle reaches a level of $\Delta\varphi = 61°$ at 10 min and, then,

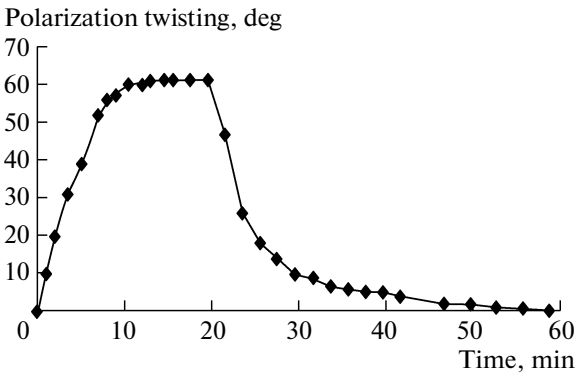


**Fig. 6.** Plot of rotation angle Δφ of the polarization plane versus time at a rotation frequency of 80 Hz. At moment $t = 20$ min, the motor is switched off to stop the rotation. The polarization recovery time is about 40 min.

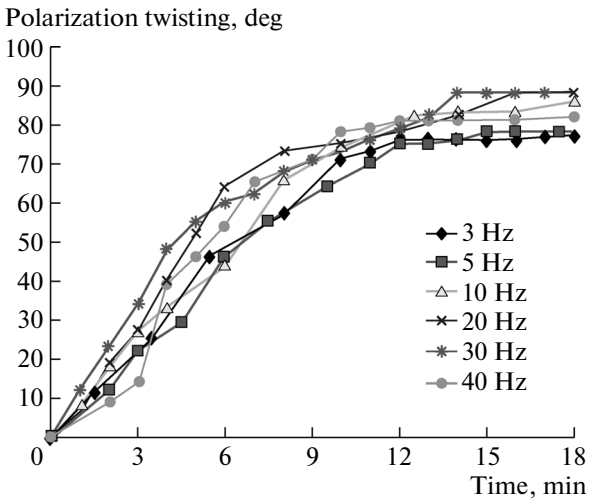


**Fig. 7.** Plot of the polarization rotation angle vs. time for the rotation frequency interval $f = 3$–40 Hz (spectral component of the vertical polarization).

remains unchanged up to the moment at which the motor is switched off (20 min). Then, the polarization returns to the initial state $\Delta\varphi = 0°$ and the recovery time is 40 min. The process can be classified as a completely reversible process.

Note that the unit containing the OD and the three-phase induction motor has dynamic stabilization, which accounts for a relatively low level of vibrations and acoustic noise (the working range of the motor frequencies is up to 400 Hz). The processing of signals that are recorded over 60 min at a constant rotation frequency of $f = 150$ Hz makes it possible to estimate the absolute error (confidence interval): $\Delta f = 0.092$ Hz. Such an error insignificantly affects the measured results. In addition, the second part of the curve in Fig. 6 is obtained for the switched-off motor after gradual stopping of rotation (the OD stopping time is 85 s) when the OD is at rest. The effect of mechanical processes (vibrations and elastic oscillations in the disk and axis precession) is completely absent. Figure 6 shows that the polarization recovery time for the OD at rest is 40 min and the process seems to be reversible. The supporting evidence was obtained in multiple measurements using the on–off switching of the disk rotation.

## DEPENDENCE OF THE POLARIZATION ROTATION ANGLE AND DEFLECTION OF THE LASER BEAM ON THE OD ROTATION FREQUENCY

In the experiments, we measure the intensity of one beam at the PD plane for the vertical polarization of the laser radiation versus the OD rotation frequencies. In the measurements at a fixed rotation frequency, we observe a transient process in the course of which the PD signal amplitude exponentially increases. After the saturation of the voltage amplitude, we rotate the polarizer to minimize the signal voltage. Then, the disk is stopped and the minimum amplitude gradually reaches the initial level. Then, the measurements are performed at different frequency $f_i$.

Figures 7 and 8 present the measured time dependences of the polarization rotation angle for the vertical initial polarization of the laser beams and two intervals of the rotation frequency ($f = 3$–40 and 50–200 Hz).

It is seen that the polarization rotation is stronger at lower frequencies.

Figure 9 shows the measured polarization rotation angles at frequencies of up to 250 Hz for the horizontal component of the laser polarization and the smoothed curve $\Delta\varphi(f)$. A similar curve is obtained for the vertical component. The measurements are performed with allowance for the transient process in the rotating OD.

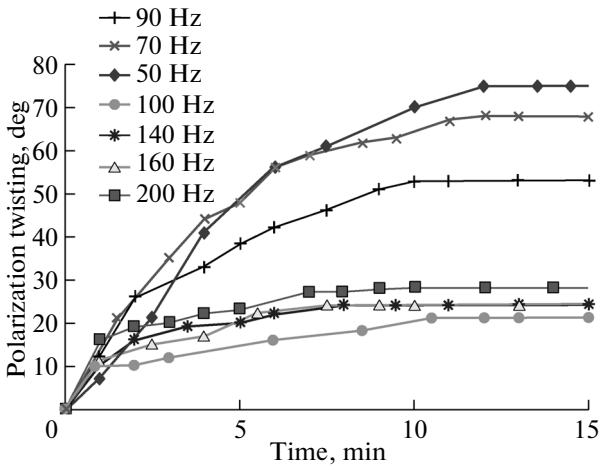


**Fig. 8.** Plot of the polarization rotation angle vs. time for the rotation frequency interval $f = 50$–200 Hz (spectral component of the vertical polarization).

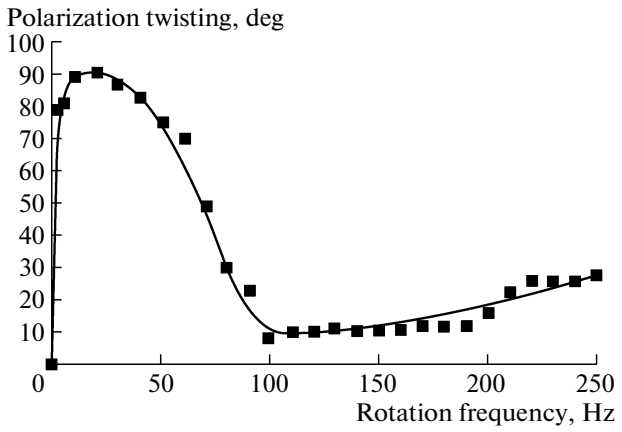


**Fig. 9.** Plot of polarization rotation angle $\Delta\varphi$ vs. rotation frequency $f$ for the horizontal spectral component of the laser (experimental results and smoothed curve).

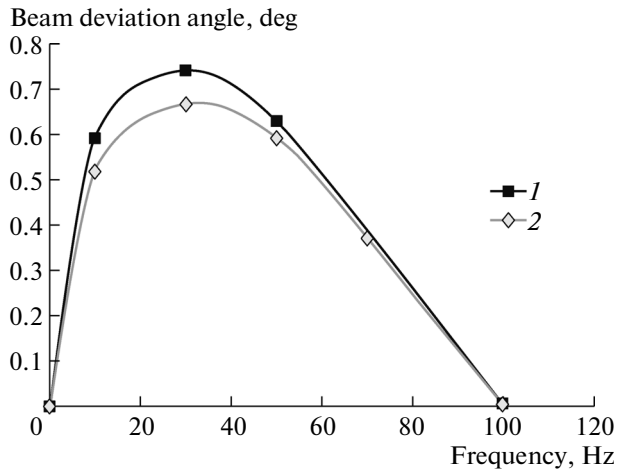


**Fig. 10.** Plots of the deflection angle of the beam having passed through the OD vs. rotation frequency $f$ for (*1*) horizontal and (*2*) vertical polarizations.

At relatively low rotation frequencies, the polarization rotation angle reaches a level of 90°. The maximum is observed at frequencies of 20–30 Hz. At rotation frequencies of 2–3 Hz, the polarization plane is rotated by an angle of $\Delta\varphi \approx 80°$.

For the frequencies $f > 100$ Hz, the rotation angle decreases to 10°–20° for both polarization components.

We also detect the deflection of the beams having passed through the rotating OD. Figure 10 presents the dependence of the deflection angle of the laser beam on the rotation frequency for two spectral components. The displacement of the light spot on the screen in the plane of observation is measured in the experiments. For the optical scheme of the experimental setup with the *OS*2 optical system, a maximum deflection angle of 0.7° corresponds to a displacement of about 10 mm on the screen.

The angular displacement of the beams on the screen in the detection plane leads to the downward vertical shift regardless of the direction of the OD rotation.

Figures 9 and 10 show maxima at a frequency of about 30 Hz. A significant difference lies in the fact that the angular deflection of the beams vanishes at frequencies of greater than 100 Hz. Note also that a transient process with a time of 10–12 min needed for reaching a steady-state level is also observed for the angular displacement of the beam at each rotation frequency. When the OD is stopped, the beam returns to the initial angular position and the corresponding characteristic times are 5 and 10 min for frequencies of 10 and 30 Hz, respectively. The time of the transient process is 3 min for frequencies of 70 and 100 Hz. The transient time for the angular displacement of the beam is not equal to the transient time of the polarization rotation. This circumstance indicates different physical processes that affect the characteristics of electromagnetic radiation propagating in the rotating OD.

## DISCUSSION

The polarization rotation and optical image in a rotating insulator have been discussed in [5–7]. It has been demonstrated that the angle of image and polarization rotation directly depend on the angular velocity.

The propagation of coherent electromagnetic radiation in a rotating insulator is accompanied by violations of the Snell law and deviations from rectilinear propagation [8, 9]. The deflection of beams that propagate in a rotating insulator in opposite directions can be significant at nonrelativistic velocities of the medium owing to the displacement of the point at which the radiation leaves the rotating disk [10].

However, the above effects and the classical Fizeau and Fermi effects follow from the solution to the Maxwell equations and linearly depend on the velocity of the medium in the first order. Conversely, the results of this work yield the nonlinear dependence of the polarization on the velocity of the medium. The experimental data show that the effect in this work substantially differs from the Fermi effect. The TF3 glass (disk material) exhibits conventional properties of the flint glass, so that the stress and birefringence that result from the industrial processing are negligibly low under normal conditions.

The initially plane-polarized radiation becomes elliptically polarized due to passage through a photoelastic medium with induced birefringence. Glass is also classified as a photoelastic material with relatively low optical sensitivity [11]. Below, we estimate the birefringence.

The generation of birefringence in the material of a rotating disk is in agreement with results of calcula-

tions at relatively high frequencies. Indeed, the phase difference of the ordinary and extraordinary beams having passed through the OD is given by

$$\varphi = \frac{2\pi l}{\lambda} B(\sigma_\theta - \sigma_r), \quad (1)$$

where $\sigma_\theta$ and $\sigma_r$ are the tangential and radial stress components, $B$ is the optical stress ratio, $l$ is the geometrical optical path in the disk, and $\lambda$ is the radiation wavelength.

For the model of a thin solid disk, the tangential and radial stress components are represented as [12]

$$\sigma_r = \frac{3+\mu}{8}\rho\omega^2(b^2 - r^2), \quad (2)$$

$$\sigma_\theta = \frac{3+\mu}{8}\rho\omega^2 b^2 - \frac{1+3\mu}{8}\rho\omega^2 r^2, \quad (3)$$

where $b$ is the external radius of the disk, $\mu$ is the Poisson coefficient, and $\rho$ is the density of glass.

The dependence of the phase difference of the ordinary and extraordinary beams having passed through the rotating OD on angular velocity $\omega$ is given by

$$\varphi(\omega) = \frac{\pi l B \rho \omega^2 (1-\mu) r^2}{2\lambda}. \quad (4)$$

For an order-of-magnitude estimation of the birefringence in glass, we use the following OD parameters: $l = 60$ mm, $r = 22$ mm (impact parameter), $B = 1.8 \times 10^{-12}$ Pa$^{-1}$, $\rho = 4.46 \times 10^3$ Ugm$^{-3}$, and $\mu = 0.221$ (TF3 glass).

For an OD rotation frequency of $f = 150$ Hz, the calculated ellipticity angle is $\varepsilon = \arctan|e| = \frac{\varphi(150\text{ Hz})}{2} = 11.43°$. On the other hand, the experimental results show that the rotation of the $\lambda/4$ retardation plate may lead to a decrease in the ellipticity by $\Delta\varepsilon = 0.2$. Assuming that such a variation is due to the compensation for birefringence, we obtain the measured ellipticity angle $\varepsilon = \arctan|\Delta e| = 11.3°$. For the frequency interval 100–200 Hz, the ellipticity angle is close to the measured polarization rotation angle and exhibits a monotonic increase. In general, dependence $\varepsilon(f)$ is similar to the experimental dependence of the polarization rotation angle on the OD rotation frequency (Fig. 9) in the entire frequency range. In other words, the polarization rotation angle correlates with the ellipticity in the frequency interval $f =$ 0–200 Hz.

A mechanical load may lead to elastic, high-elasticity, and residual deformation in nonmetal materials. As distinct from the elastic deformation, the high-elasticity deformation vanishes with a certain delay after unloading. Time dependences in Figs. 5–8 can be interpreted using such a deformation. The external mechanical field that is caused by rotation leads to a decrease in the potential barriers, and the molecules that are involved in the thermal motion may exhibit flexibility that provides the generation and development of reversible high-elasticity deformations.

Note that the relaxation time of glass properties ($\tau = 10^2$–$10^3$ s) is significantly greater than time $\tau = 10^{-12}$–$10^{-14}$ s that is typical of dielectric materials [13–15]. The results of Figs. 7 and 8 make it possible to qualitatively estimate the time dependence of the high-elasticity deformation of glass. These results show that the time dependence of the polarization rotation angle can be represented as

$$\varphi(f) = \varphi_0(f)\left(1 - e^{-\frac{t}{n(f)}}\right), \quad (5)$$

where $\varphi_0(f)$ is the polarization rotation angle at frequency $f$ at $t \longrightarrow \infty$ and $n(f)$ is the numerical coefficient, which is $n \approx 10$ ($\approx 1$) for $f < 80$ Hz ($f > 100$ Hz).

The beam deflection (Fig. 10) can be interpreted using the generation of a gradient of refractive index owing to the generation of stress in the material of rotating disk. A variation in the refractive index along the tangential direction can be estimated using expression (3) as

$$\Delta n_\theta = B_{\sigma_\theta} = \frac{B\rho\omega^2}{8}[(3+\mu)b^2 - (1+3\mu)r^2]. \quad (6)$$

Substituting the parameters that characterize the glass material, we obtain $\Delta n_\theta = 9 \times 10^{-7}$ for a frequency of $f = 100$ Hz. Such a variation in the refractive index is beyond the measurement accuracy of the experiments. In addition, Fig. 10 shows the absence of deflection at high frequencies.

In general, we conclude that the birefringence and deformation at frequencies $f > 100$ Hz are in agreement with modern concepts of the behavior of loaded amorphous objects. Nonlinear effects in the frequency interval 0–100 Hz were tested using three ODs made of the TF3 glass. The measurements yield the absence of the dependence of the above effects on the laser power for the coherent source of the experimental setup. In particular, the measured polarization rotation for the rotating OD remains unchanged after long-term blocking of the radiation. It is expedient to study the polarization using a system in which the laser radiation interacts with a rotating optically transparent medium in different spectral ranges at higher radiation powers.

## CONCLUSIONS

The experiments using the steady-state rotation of the OD yield the evolution of polarization that involves relatively long transient process of the polarization rotation and variations in the ellipticity and degree of polarization. The transient time depends on the OD rotation frequency and amounts to 15–20 min for frequencies ranging from 0 to 200 Hz. The observed processes are completely reversible.

The time dependences and the reversible character of elastic deformations seemingly point to high-elasticity deformations in the material of the rotating disk.

In the entire interval of rotation frequencies $f$, the dependence of ellipticity angle $\varepsilon(f)$ is qualitatively similar to the experimental dependence of the polarization rotation angle on the OD rotation frequency.

We have also detected the angular deflection of the beams having passed through the rotating OD. Note that the switching of the direction of the OD rotation does not lead to significant variations in the polarization rotation, ellipticity, degree of polarization, and beam deflection at fixed rotation frequencies.

The results of this work could not have been obtained in [2] in which the experiments employed a cylinder with a relatively small diameter and the radiation was incident almost along the normal on the end surface.

Finally, note the practical importance of the observed dependence of the characteristics of laser radiation on disk rotation velocity. Rotation angle $\Delta\varphi$, ellipticity $e$, and degree of polarization $p$ depend on the optical parameters of the moving medium. Therefore, the measurement of such parameters can be used to additionally characterize the medium. For example, the rotation-induced signal can be used to study the spatial spectrum of the distribution of inhomogeneities in the disk material. The fact that opposite polarization rotations are obtained for the beams that pass through the rotating disk in opposite directions is important for practical applications, since the effect can be used for the control of laser radiation. It is of interest to study the processes at various angles of incidence using several optical materials.

## ACKNOWLEDGMENTS

We are grateful to V.D. Shargorodskii and S.I. Makretsov for the assistance in fabrication of optical disks and experiments.

## REFERENCES

1. E. Fermi, Rend. Lincei **32**, 115 (1923).
2. R. V. Jones, Proc. R. Soc. London, Ser. A: Math. Phys. **349**, 423 (1976).
3. V. O. Gladyshev, D. I. Portnov, V. L. Kauts, and E. A. Sharandin, Opt. Spectrosc. **115**, 349 (2013).
4. V. O. Gladyshev, P. S. Tiunov, A. D. Leont'ev, T. M. Gladysheva, and E. A. Sharandin, Tech. Phys. **57**, 1519 (2012).
5. M. Padgett, G. Whyte, J. Girkin, A. Wright, L. Allen, P. Ohberg, and S. M. Barnett, Opt. Lett. **31**, 2205 (2006).
6. L. Allen and M. Padgett, J. Mod. Opt. **54**, 487 (2007).
7. S. Franke-Arnold, G. Gibson, R. W. Boyd, and M. J. Padgett, Science **333**, 65 (2011).
8. V. O. Gladyshev, JETP Lett. **58,** 569 (1993).
9. N. N. Rozanov and G. B. Sochilin, Phys. Usp. **49**, 407 (2006).
10. V. O. Gladyshev, Tech. Phys. **44**, 566 (1999).
11. K. Vollrath and G. Thomer, *Kurzzeitphysik/Physique des Phenomenes Ultra-Rapides/High-Speed Physics* (Springer, Wien, 1967).
12. S. P. Timoshenko and J. N. Goodier, *Theory of Elasticity,* 3rd ed. (McGraw-Hill, New York, 1970).
13. G. O. Karapetyan, Yu. G. Korolev, L. V. Maksimov, and S. V. Nemilov, Fiz. Khim. Stekla **12**, 598 (1986).
14. N. F. Borrelli and W. H. Dumbaugh, Proc. SPIE **843**, 6 (1987).
15. N. F. Borrelli, B. G. Aitken, M. A. Newhouse, and D. W. Hall, J. Appl. Phys. **70**, 2774 (1991).

*Translated by A. Chikishev*